Published in final edited form as:
Dev Biol. 2007 June 1; 306(1): 208–221. doi:10.1016/j.ydbio.2007.03.018.

The *Hectd1* Ubiquitin Ligase is Required for Development of the Head Mesenchyme and Neural Tube Closure

Irene E. Zohn[1,^], **Kathryn V. Anderson**[2], and **Lee Niswander**[1,*]

[1]Howard Hughes Medical Institute, Department of Pediatrics, Section of Developmental Biology, University of Colorado at Denver and Health Sciences Center, Aurora, Colorado, 80045, USA

[2]Developmental Biology Program, Sloan-Kettering Institute, New York, New York, 10021, USA

Abstract

Closure of the cranial neural tube depends on normal development of the head mesenchyme. Homozygous-mutant embryos for the ENU-induced *open mind* (*opm*) mutation exhibit exencephaly associated with defects in head mesenchyme development and dorsal-lateral hinge point formation. The head mesenchyme in *opm* mutant embryos is denser than in wildtype embryos and displays an abnormal cellular organization. Since cells that originate from both the cephalic paraxial mesoderm and the neural crest populate the head mesenchyme, we explored the origin of the abnormal head mesenchyme. *opm* mutant embryos show apparently normal development of neural crest-derived structures. Furthermore, the abnormal head mesenchyme in *opm* mutant embryos is not derived from the neural crest, but instead expresses molecular markers of cephalic mesoderm. We also report the identification of the *opm* mutation in the ubiquitously expressed *Hectd1* E3 ubiquitin ligase. Two different Hectd1 alleles cause incompletely penetrant neural tube defects in heterozygous animals, indicating that Hectd1 function is required at a critical threshold for neural tube closure. This low penetrance of neural tube defects in embryos heterozygous for Hectd1 mutations suggests that Hectd1 should be considered as candidate susceptibility gene in human neural tube defects.

Introduction

The central nervous system of the vertebrate embryo originates during gastrulation with the formation of the neural plate. During subsequent development, the neural plate undergoes extensive morphogenic movements resulting in formation of the neural tube. When the neural tube fails to close completely during its morphogenesis, neural tube defects result. Neural tube defects are one of the most common human congenital malformations occurring in approximately one out of every one thousand live births (Copp et al., 2003; Zohn et al., 2005). Common forms of neural tube defects include spina bifida and exencephaly where the neural tube remains open in the most caudal and rostral aspects of the neural axis, respectively. In humans, neural tube defects represent a complex disease with multiple environmental and genetic contributing factors. Because of the multifaceted etiology of human neural tube defects, identification of causative mutations has been problematic.

*Correspondence to Lee Niswander, University of Colorado Health Sciences Center - Fitzsimmons Campus, Department of Pediatrics, PO Box 6511, MS 8322, 12800 E. 19th Ave., Aurora, CO 80045, USA, email: Lee.Niswander@UCHSC.edu.
^Present address: Center for Neuroscience Research, Children's Research Institute, Children's National Medical Center, Washington, DC 20010, USA

Vertebrate model systems have been indispensable for the discovery of the processes required for neural tube closure. The mouse has been particularly useful for identification of genes required for proper morphogenesis of the neural tube and the generation of numerous mouse models for neural tube defects has implicated a long list of candidate genes for human neural tube defects (Copp et al., 2003; Zohn et al., 2005). These genes regulate cell movement, apoptosis, proliferation, patterning and differentiation of not only the neural tissue, but also the surrounding mesenchyme and non-neural ectoderm. Moreover, in some cases, identification of key regulators of neural tube closure in mice has helped to uncover the genetic basis of neural tube defects in humans (Gelineau-van Waes and Finnell, 2001).

Neural tube closure is a complex morphogenic process where the neural plate rolls into a tube forming the central nervous system (Copp et al., 2003; Zohn et al., 2005). The neural folds form at the edges of the neural plate and rise towards the dorsal midline due to forces from both the neural tissue and the surrounding epithelium and mesenchyme. Apical constriction of cells in the midline and in more lateral regions results in the formation of medial and dorsal-lateral hinge points respectively. In the cranial neural tube, neural fold elevation is accompanied by an expansion of the head mesenchyme (Morriss and Solursh, 1978) and reviewed in (Copp, 2005). This expansion is mediated by both increased cell proliferation and an increase in the extracellular space between the mesenchymal cells and is thought to be critical to allow the elevation of the neural folds. The molecular signals regulating these cellular behaviors of the head mesenchyme remain unknown.

Cells that originate from both the cephalic paraxial mesoderm and the neural crest populate the head mesenchyme (Noden and Trainor, 2005). The cephalic mesoderm is derived from the cells in the primitive streak immediately caudal to the node. As gastrulation progresses, cells from the paraxial mesoderm spread medio-laterally from the primitive streak to a position beneath the developing neural plate. In contrast, the cranial neural crest is derived from cells that are located at the junction of the neural and non-neural ectoderm. Once specified, neural crest cells migrate ventral-laterally between the surface ectoderm and the paraxial mesoderm. During later stages of development, the paraxially-derived cephalic mesoderm contributes to multiple structures such as the smooth and skeletal muscles and some of the cartilaginous and bony elements of the skull. The neural crest contributes to cranial nerves, blood vessels and many of the bony elements of the head and face.

Cranial neural tube closure is critically dependent on the proliferation and cellular rearrangement of the head mesenchyme. Mouse models with deletions in the *Twist1*, *Cart1* or *Tcfap2a* genes exhibit cranial neural tube closure defects linked to defects in development of the head mesenchyme (Chen and Behringer, 1995; Schorle et al., 1996; Zhang et al., 1996; Zhao et al., 1996). *Twist1* function is required in the head mesenchyme where it is expressed in both the paraxial mesoderm and the neural crest lineages (Chen and Behringer, 1995). Yet it is unknown if either *Twist1* or *Cart1* are required in the mesoderm or neural crest or both lineages. Deletion of *Tcfap2a* specifically in the neural crest results in exencephaly, indicating that *AP-2α* function in the neural crest is essential for cranial neural tube closure (Brewer et al., 2004).

Here we describe the further characterization of the neural tube defects in the ENU-induced *open mind* (*opm*) mutant mouse line. Homozygous *opm* mutant embryos exhibit severe defects in cranial neural tube closure (Kasarskis et al., 1998). We demonstrate that the neural tube closure defect in *opm* mutant embryos is associated with a failure of dorsal-lateral hinge point formation and an abnormal organization of the head mesenchyme surrounding the neural tube during closure. In spite of the severe defects in cranial neural tube closure and the abnormal head mesenchyme, *opm* mutant embryos exhibit apparently normal development of neural crest-derived structures such as facial bones and palate. Neural crest development also appears

normal in *opm* mutant embryos as assayed by both molecular marker and lineage-tracing analysis. In contrast, analyses of the expression pattern of molecular markers that mark the cephalic mesoderm suggest that this tissue is abnormally dense in *opm* mutants. By positional cloning we identify the *opm* mutation in an uncharacterized ubiquitin ligase (*Hectd1*) that is ubiquitously expressed throughout early development of the mouse embryo. Our data also indicate that a critical threshold of Hectd1 function is required for neural tube closure as up to 20% of mutant heterozygotes exhibit neural tube defects depending on the mutant allele. The low penetrance of neural tube defects in heterozygous embryos suggests that Hectd1 should be considered as a candidate susceptibility gene in human neural tube defects.

Materials and Methods

Analysis of mutant phenotype

Whole-mount and section RNA in situs were performed as described (Holmes and Niswander, 2001; Liu et al., 1998) using the following probes: *Fgf8* (Crossley and Martin, 1995), *BMP4* (Jones et al., 1991), *Sox10* (Pusch et al., 1998), *AP-2α* (Mitchell et al., 1991), *Tbx1* (Chapman et al., 1996), *Snail* (Nieto et al., 1992), *Twist* (Chen and Behringer, 1995), *PDGFRα* (Schatteman et al., 1992). The expression pattern of *Hectd1* was determined using an anti-sense RNA probe synthesized from IMAGE clone: 3672615 or determining LacZ activity in $Hectd1^{XC/+}$ embryos. For immunofluorescence experiments, embryos were dissected from the decidua and fixed for 1 hour in 4% paraformaldehyde in PBST (Phosphate-buffered saline (PBS) plus 0.1% Tween-20), washed 3 times in PBST, cryopreserved in 30% sucrose in PBS, embedded in OCT compound (Tissue-Tek) and sectioned at 10 μM. Fixed frozen sections were processed as described (Timmer et al., 2002) using the anti-phospho-Histone H3 Mitosis Marker (1:250; Upstate Biotechnology) for proliferation assays or the cleaved Caspase-3 antibody (1:250; Cell Signaling #9661) for apoptosis assays. Sections were mounted with Vectashield mounting medium with DAPI (Vector Laboratories; H-1200) or stained with Hoechst (10 μg/ml; Sigma) to stain nuclei and allow counts of the total number of cells. For Hematoxylin and Eosin staining, embryos were fixed overnight in 4% paraformaldehyde in PBST and processed for frozen sectioning as described (Timmer et al., 2002). Skeletal and β-galactosidase staining were performed as described (Hogan et al., 1994).

Mouse Strains and Genotyping

The *opm* mouse line was identified in a screen for recessive ENU-induced mutations that cause defects in neural tube closure at E9.5 (Garcia-Garcia et al., 2005; Kasarskis et al., 1998; Zohn et al., 2005). The *opm* mutation was generated on a C57BL/6J genetic background and backcrossed to C3H/HeJ for at least 10 generations to obtain a congenic line. The mapping of the opm mutation was done during the creation of the congenic line, while the high resolution mapping data was generated once the congenic line (e.g. >N10) was established. Approximately 5% of *opm*/+ embryos exhibit defects in cranial neural tube closure (see Table 1). However, the neural tube defect in these heterozygous embryos is less severe (only mid- and hindbrain exencephaly) and can be easily distinguished at E9.5 and E10.5 from *opm/opm* embryos (exencephaly from the forebrain to the hindbrain). For this reason, mapping of the *opm* mutation was done using only E9.5 and E10.5 embryos from crosses of *opm*/+ females mated to *opm*/+ males. In a mapping cross of 590 opportunities for recombination, *opm* was mapped between the Massachusetts Institute of Technology (MIT) simple sequence length polymorphism (SSLP) markers D12mit64 and D12mit54 with no recombination with D12mit110. For high-resolution mapping, additional polymorphic DNA markers were generated based on nucleotide repeat sequences and include: D12ski18, D12ski16 and D12ski12 (see http://mouse.ski.mskcc.org/ for sequence of primers).

The entire *Hectd1* transcript was sequenced by RT-PCR (Superscript One-Step RT-PCR, Invitrogen) using RNA isolated from E10.5 *opm/opm* and C57BL/6 control embryos. At position 430, a T to A transversion was discovered in the 7833 base pair open reading frame that encodes *Hectd1*. This mutation results in a nonsense mutation changing a Leucine to a stop codon at amino acid 145 in the predicted 2611 amino acid Hectd1 protein.

A mouse embryonic stem (ES) cell line carrying an insertion in the *Hectd1* gene (XC266) was identified from a blast search using the *Hectd1*-coding sequence against the BayGenomics (http://baygenomics.ucsf.edu/) database (Skarnes et al., 2004). Mice carrying the *Hectd1* insertion were generated by standard blastocyst injection followed by breeding for at least two generations into a C3H background and named *Hectd1*^{XC}. Mice carrying the genetrap allele were genotyped using *LacZ*-specific primers (Liu et al., 1998). Other mouse strains used were *Wnt1-Cre* (Danielian et al., 1998) and the *R26R* conditional reporter allele (Soriano, 1999).

Results

opm mutant embryos exhibit exencephaly

In our ongoing ENU mutagenesis screens to identify genes that are required for neural tube closure (Zohn et al., 2005), we isolated the *open mind* (*opm*) mutant mouse line (Kasarskis et al., 1998). This mouse mutant is distinct from the ENU-induced *openmind* (*om*) mouse mutant, which harbors a mutation in the *Rere/atrophin-2* gene (Zoltewicz et al., 2004). As summarized in Table 1, Mendelian ratios of *opm/opm* mutant embryos are recovered with exencephaly upon dissection at E9.5-E12.5. Additionally, approximately 5% of heterozygous embryos show a less severe exencephaly affecting only the midbrain and hindbrain (Table 1 and data not shown). Homozygous *opm* mutant embryos display exencephaly characterized by a failure of neural tube closure from the hindbrain to the forebrain. The closure point at the most anterior aspect of the forebrain is typically closed, but in some embryos this closure point remains open resulting in a split of the facial primordia down the midline at E9.5 although this appears to resolve as we do not detect cranial-facial defects at later stages (Figure 1A-L; see below and data not shown (Kasarskis et al., 1998). Eye morphogenesis is also affected as *opm* mutant eyes are malformed, smaller and are rotated in the head (Figure 1O, P).

In spite of the severe defects in neural tube closure in *opm* mutant embryos, other aspects of cranial-facial development appear to be unaffected. The facial primordial consists of the frontonasal prominence and the first branchial arch. Around day 10, the nasal placodes in the frontonasal prominence invaginate resulting in formation of the medial and lateral nasal prominences (Kaufman and Bard, 1999). As shown in Figure 1G-H, *Fgf8* is expressed in the ectoderm of the nasal pits and the medial nasal process and is expressed in a similar domain in both *opm* mutant and wildtype embryos. By E11.5, the medial and lateral prominences fuse to form the nasal pits as highlighted by *Bmp4* expression (Figure 1K). In the developing face of *opm* mutant embryos, *Bmp4* is expressed in a similar domain as in wildtype (Figure 1L). The secondary palate forms from outgrowths of the medial walls of the maxillary prominence, which fuse in the midline with the nasal septum. Coronal sections of E14.5 wildtype and mutant heads reveals that the secondary palatal shelves fuse normally in *opm* mutant embryos (Figure 1M, N). These results indicate that unlike other mouse mutants which exhibit similar neural tube closure defects from the forebrain to the hindbrain such as *Twist1*, *Cart1* or *Tcfap2a* (Chen and Behringer, 1995; Schorle et al., 1996; Zhang et al., 1996; Zhao et al., 1996), the facial primordia are able to undergo proper morphogenesis in *opm* mutant embryos.

To further examine the effect of the *opm* mutation on cranial-facial growth, development of the facial skeleton was examined later in development (E17.5). As shown by the gross morphology of the face of *opm* mutant embryos (Figure 1Q-T), the face and snout of mutant embryos develops normally. Skeletal staining reveals that *opm* mutant embryos exhibit some

malformations in the growth of the skull vault such as abnormally shaped frontal and parietal bones (arrowheads in Figure 1V) and the absence of the exoccipital, petrosal and interpariatal bones (* in Figure 1V); however, these malformations are likely a secondary result of the cranial neural tube closure defect (Copp, 2005). Aside from these malformations, this analysis does not reveal any other gross morphological defects in development of the cranial-facial skeleton (Figure 1U-X). Therefore, unlike other mutants with similar neural tube defects such as *Twist*, *CART1* and *Tcfap2a*, craniofacial development of structures rostral to the open neural tube is normal in *opm* mutants.

Cranial neural tube closure defects in *opm* mutant embryos are associated with defects in development of the head mesenchyme

The failure of neural fold elevation and the open neural tube from the forebrain to the hindbrain is strikingly similar to the neural tube defects observed in *CART1* and *Twist* mutant embryos (Chen and Behringer, 1995; Zhao et al., 1996). Previous studies have implicated the involvement of these genes in proper development of the head mesenchyme. Therefore, histological analysis was used to investigate whether the head mesenchyme is affected in *opm* mutants. Coronal sections of wildtype and *opm* mutant heads were stained with hematoxylin and eosin to reveal the cellular organization of the head mesenchyme surrounding the neural tube (Figure 2A-D). This analysis demonstrates that the head mesenchyme in *opm* mutants is abnormal and appears to be denser around the open neural tube (Figure 2B,D). To further quantify the density of the head mesenchyme cells, the number of head mesenchyme cells in identical areas of wildtype and mutant heads in many embryos were counted to obtain cell densities. Since an increased cell density could result from a failure of neural fold elevation, areas of head mesenchyme were selected ventral to the dorsal-lateral hinge points such as those in the boxed regions of Figure 2A and C. The density of cells in the head mesenchyme of E9.5 mutant embryos were significantly ($p < 0.0001$) greater than in wildtype embryos as determined by the Mann-Whitney U test (Figure 2I). Furthermore, the increased cell density is observed early as the neural folds are beginning to elevate (e.g. at E8.5). This is in contrast to our earlier findings suggesting that the mesenchyme was less dense (Kasarskis et al., 1998). After our current careful analysis, our previous observation now appears to be an artifact of the plane of few sagittal sections. We also observed an increase in the thickness of the head mesenchyme around the dorsal and lateral aspects of the neural tube in mutant versus wildtype embryos (Figure 2A,C,E,F brackets). This expansion of head mesenchyme is not seen in other mouse mutant lines with exencephaly from our screens. For example, neural tube defects in the *humdy* mutant mouse line are associated with an increase in the proliferation of neural tissue (Taehee Kim and Lee Niswander, submitted). Furthermore, the head mesenchyme is not denser in *humdy* mutants indicating that abnormal head mesenchyme is not always secondary to failure of neural tube closure. These findings indicate that the *opm* phenotype is associated with an abnormal organization of the head mesenchyme around the cranial neural tube.

In order to determine if the abnormal organization of head mesenchyme in *opm* mutant embryos occurs before cranial neural tube closure, the head mesenchyme was examined at a stage that precedes this event. Coronal sections of embryos at E8.5 (12 somites; Figure 2G,H) were stained with Hoechst to highlight the morphology of the tissue. As indicated by brackets in Figure 2G,H, these defects precede cranial neural tube closure as the thickness of the head mesenchyme around the neural tube is already increased at this stage. Additionally, quantification of cell density in the head mesenchyme of E8.5 embryos indicates that there is a significant difference ($p<0.0001$; Mann-Whitney U test) between the density of cells in wildtype and mutant embryos even before neural tube closure (Figure 2I). Since, the increase in cell density precedes neural tube closure, it is unlikely due to the failure of neural tube closure. Taken together, these results suggest that the neural tube defect in *opm* mutant embryos

could be due (at least in part) to the abnormal organization and increased density of the head mesenchyme surrounding the neural tube during neural fold elevation and neural tube closure.

Another mechanistic defect that can lead to neural tube defects is a failure to form the hinge points, which facilitate the convergence of the neural folds in the dorsal midline. The medial hinge point forms normally in *opm* mutant embryos (Figure 2A-H), consistent with normal dorsal-ventral patterning of the neural tissue (data not shown), both processes which are known to be regulated by Shh signaling (Caspary and Anderson, 2003; Ybot-Gonzalez et al., 2002). In contrast, the dorsal-lateral hinge points completely fail to form in *opm* mutants (arrows; Figure 2A-H), resulting in a flat or convex curvature of the neural tissue rather than the concave and closed neural tube seen in wildtype embryos (Figure 1C,D and Figure 2A-F).

To determine if the dense head mesenchyme results from changes in cell proliferation or apoptosis, these processes were examined in E8.5 and E9.5 embryos, prior to and during the time of cranial neural closure. Apoptosis was examined using the cleaved caspase-3 antibody, which marks cells that are initiating apoptosis. In wildtype and mutant embryos, very few cells were undergoing apoptosis in the head mesenchyme surrounding the neural tube (data not shown). Therefore it is unlikely that differences in apoptosis are responsible for the dramatic differences in the number of cells populating the head mesenchyme of wildtype and *opm* mutant embryos. Proliferation was measured by examining expression of phosphorylated-Histone-3 (P-H3), which increases during mitosis. To assess the rate of proliferation, the number of P-H3 positive cells were counted and divided by the number of cells in a given area of the head mesenchyme to give a mitotic index as shown in Figure 2J. To determine if mitotic indexes are significantly different in *opm* mutant versus wildtype head mesenchyme, the Mann-Whitney U test was used. For E8.5 and E9.5 wildtype versus *opm* mutants the p-value was 0.1980 and 0.9552, respectively. These results indicate that there are no significant differences in the mitotic indexes of the abnormal head mesenchyme surrounding the neural tube in *opm* mutant embryos as compared to control littermates.

opm mutant embryos do not exhibit defects in neural crest cell development

Our data indicate that neural tube defects in opm mutant embryos are associated with defects in development of the head mesenchyme. Additionally, the open neural tube phenotype of *opm* mutants is reminiscent of the neural tube defects exhibited by *Twist* and *AP-2α* mutants (Chen and Behringer, 1995; Schorle et al., 1996; Zhang et al., 1996; Zhao et al., 1996), which also exhibit severe defects in the development of the head mesenchyme. Since the head mesenchyme is composed of cells that are of both neural crest and mesoderm origin (Noden and Trainor, 2005), the head mesenchyme defect in *opm* mutant embryos could originate from either source. Therefore, we sought to determine the origin of the abnormal head mesenchyme using a molecular marker analysis. If the abnormal head mesenchyme is due to defects in neural crest cell development, this should be evident by examination of neural crest specific markers at early developmental stages. Examination of *Sox10* and *AP-2α* expression at E8.5 indicated that neural crest induction and its initial migration are normal in *opm* mutant embryos (Figure 3A-D). Additionally, expression of *Sox10* and *AP-2α* at E9.5 indicates that the neural crest migrates and undergoes its initial differentiation normally (Figure 3E-H). Lastly, the expression of *AP-2α* at E9.5 indicates that the neural crest does not contribute to the regions of abnormal mesenchyme of *opm* mutants (* in Figure 3H). This normal initial development of neural crest derived structures in *opm* mutant embryos agrees with our observations that later in development, neural crest-derived structures such as the facial bones and palate develop normally in *opm* mutants (Figure 1M-X).

To further explore a potential contribution of neural crest cells to the abnormal head mesenchyme in *opm* mutants, genetic fate-mapping experiments were performed. For these experiments, the *opm* mutation was crossed into the *Wnt1-Cre* and *R26R* transgenic mouse

strains (Danielian et al., 1998; Soriano, 1999). As shown in Figure 3I,J, E9.5 *opm* mutant embryos exhibit normal development of *Wnt1*-lineage traced cells in the head mesenchyme. In fact, the abnormally dense tissue surrounding the neural tube in *opm* mutant embryos is LacZ-negative (* in Figure 3J). This is better visualized in coronal sections where it is evident that cells of neural crest origin do not populate the abnormal head mesenchyme surrounding the open neural tube and migrate to the correct position in the developing heads of *opm* mutant embryos (Figure 3K,L). Thus, this lineage tracing experiment clearly indicates that it is not of neural crest origin (brackets in Figure 3K,L).

Molecular markers of cephalic mesoderm

The results described above indicate that the abnormal head mesenchyme surrounding the open neural tube in *opm* mutants is not derived from the neural crest. Therefore, we next sought to determine if this head mesenchyme is derived from the cephalic mesoderm. To do so, the expression of a number of molecular markers of cephalic mesoderm was examined. *Tbx1* is expressed in the caudal cephalic mesoderm and the mesoderm that populates the branchial arches. Examination of *Tbx1* in wildtype and *opm* mutant embryos at E9.5 and E8.5 indicates that its expression domain is not expanded in *opm* mutant embryos (Figure 4A-D). In contrast, in situ hybridization analysis at E9.5 using antisense probes against *Snail*, *Twist* and *PDGFRα*, molecular markers of both cranial neural crest and mesoderm, indicates that the abnormal head mesenchyme in *opm* mutant embryos expresses these markers (Figure 4E-J). Since the head mesenchyme is partially obscured by exencephalic neural tissue in the whole mount in situs, expression of *Twist* and *PDGFRα* was also visualized in coronal sections. Examination of section in situs clearly shows that the expression domain of both *Twist* and *PDGFRα* is expanded in *opm* mutant heads (Figure 4K-N). This is not simply due to the exencephaly, as mouse mutants that have exencephaly associated with, for example, defects in the organization of actin in the neural tissue do not show this expansion of *Twist* surrounding the neural tube (Hildebrand and Soriano, 1999). At E8.5, the expression of *Snail* in the abnormal head mesenchyme in *opm* mutant embryos is less evident. However, *Twist* appears to be expressed in an expanded domain at this stage (Figure 4O-R, *). These results combined with our analysis of neural crest cell fate indicates that the abnormal head mesenchyme associated with the cranial neural tube closure defects in *opm* mutant embryos is derived from the cephalic mesoderm rather than the neural crest and that this defect occurs as early as E8.5.

The *opm* mutation disrupts a HECT domain ubiquitin ligase

Using positional cloning techniques, the *opm* mutation was mapped to a 1.7 MB interval on mouse chromosome 12 that contains 12 genes (Figure 5A). One interesting candidate was a novel ubiquitin ligase (*Hectd1*) with a Hect-domain (Homologous to E6-AP Carboxy Terminal). Hect-domain ubiquitin ligases mediate transfer of ubiquitin and target substrate proteins for either degradation or modification of activity (Kerscher et al., 2006). Upon sequencing, a point mutation was identified in the *Hectd1* gene (Figure 5B). The mutation results in a T to A transversion and a change of a Leucine to a stop codon after amino acid 144 in the predicted 2611 amino acid Hectd1 protein (predicted molecular weight of 289 KD). The Hectd1 protein contains a number of conserved protein domains (Figure 5G): an ankyrin repeat in the N-terminal portion of the protein likely mediates protein-protein interactions; a central mind bomb (mib) domain and a C-terminal HECT domain. These domains are also present in a number of E3 ubiquitin ligases. The *opm* mutation results in truncation of the Hectd1 protein before any of these conserved domains and likely represents a null allele (Figure 5G).

To confirm that this mutation in *Hectd1* is responsible for the developmental defects observed in the *opm* mutant line, a second allele was obtained from the BayGenomics genetrap resource (Skarnes et al., 2004). The genetrap allele, $Hectd1^{XC}$, consists of a LacZ-Stop cassette inserted into the HECT domain (Figure 5G). A complementation test was done to confirm that the

Hectd1 mutation in the *opm* mouse line is responsible for the observed phenotypes. Embryos were generated that consist of the genetrap allele over the *opm* allele ($Hectd1^{XC/opm}$) and the phenotype in mutant embryos was examined at E9.5. $Hectd1^{XC/opm}$ embryos exhibit exencephaly that is identical to that observed in *opm* homozygous mutant embryos (Figure 5C-F). Moreover, the phenotype of $Hectd1^{XC/XC}$ mutant embryos was identical to that of $Hectd1^{opm/opm}$ mutants (data not shown and Table 2). Interestingly, embryos heterozygous for the $Hectd1^{XC}$ allele exhibited exencephaly at a much higher frequency (8/40 = 20% of embryos) than $Hectd1^{opm/+}$ embryos, which exhibit exencephaly in only 5% of cases, indicating a weak dominant-negative effect of the $Hectd1^{XC}$ allele (compare Tables 1 and 2). These results confirm that the point mutation identified in the *Hectd1* gene is responsible for the phenotypes observed in *opm* mutants. Furthermore, the observation that disruption of the HECT domain produces the same neural tube closure defect phenotype as the null allele indicates that the ubiquitin ligase activity of Hectd1 is essential for its biological function.

Expression of the *opm* gene during embryogenesis

We examined the expression pattern of *Hectd1* during neurulation in $Hectd1^{XC}$ embryos that expresses the *βgeo* reporter under the endogenous *Hectd1* promoter. In phenotypically normal $Hectd1^{XC/+}$ embryos, *Hectd1:βgeo* was expressed ubiquitously during gastrulation and neurulation (Figure 6). Importantly, LacZ activity was detected in the developing head mesenchyme, consistent with a role for *Hectd1* in development of this tissue (Figure 6C-F). Additionally, LacZ activity was detected in the placenta (Figure 6G), and at higher levels in other developing tissues such as the lens of the eye (Figure 6H), the differentiated neurons in the spinal neural tube (Figure 6I) and the atrium of the heart (Figure 6J).

Discussion

Neural tube closure defects are common developmental malformations that result in death or long-term physical disabilities in humans. Here we show that an ENU-induced mutation in the *open mind* (*opm*) mutant mouse line disrupts the gene encoding the uncharacterized Hectd1 ubiquitin ligase. The cranial neural tube of *opm* mutant embryos fails to undergo proper morphogenesis and is open from the forebrain to the hindbrain. This neural tube defect is accompanied by an increase in the density and abnormal organization of the head mesenchyme surrounding the open neural tube, as well as failure to form the dorsal-lateral hinge points. Neural crest development in *opm* mutant embryos is apparently normal as determined by development of neural crest-derived structures. Additionally, molecular marker and lineage-tracing analysis during the induction and migration of the neural crest indicates that these processes occur normally in *opm* mutants. In contrast, the abnormal head mesenchyme expresses molecular markers of cephalic mesoderm indicating that *Hectd1* is required for normal development of this lineage. Finally, the low penetrance of neural tube defects in *Hectd1* mutant heterozygotes indicates that the level of *Hectd1* gene activity is critical for proper closure of the neural tube.

Mechanism of cranial neural tube closure defects in opm mutant embryos

During cranial neural tube closure, the head mesenchyme undergoes expansion by increasing both cell proliferation and the extracellular space between mesenchymal cells (Morriss and Solursh, 1978). This expansion is thought to be required for elevation of the neural folds (Copp, 2005; Copp et al., 2003). Neural fold elevation is also mediated by bending of the neuroepithelium through apical constriction resulting in the formation of the medial and dorsal-lateral hinge points (Copp, 2005; Copp et al., 2003). Together these forces convert the flat neural plate to a concave morphology contributing to the convergence of the neural folds in the dorsal midline and their subsequent fusion. The cranial neural tube in *opm* mutant embryos exhibits a complete failure of dorsal-lateral hinge point formation and neural fold elevation.

Furthermore, expanded and denser head mesenchyme around the cranial neural tube during closure accompanies this failure in neural fold elevation.

Genetic evidence that cranial neural tube closure is dependent on the proper expansion of the head mesenchyme is supported by studies of the *Twist* and *CART1* mutant phenotypes (Chen and Behringer, 1995; Zhao et al., 1996). Like *opm* mutant embryos, *Twist* and *CART1* mutants exhibit failures of cranial neural fold elevation. However, rather than the increase density of head mesenchyme observed in *opm* mutant embryos, *Twist* and *CART1* mutants exhibit a decrease in the density of head mesenchyme cells due to decreased cell proliferation and increased apoptosis, respectively (Chen and Behringer, 1995; Zhao et al., 1996). In contrast, our data do not indicate a statistically significant change in proliferation or apoptosis of the head mesenchyme during neurulation in *opm* mutants. Furthermore, we show through both lineage tracing and molecular marker analysis that the abnormal head mesenchyme is not derived from the cranial neural crest but instead from the cephalic mesoderm. Below we suggest possible molecular and cellular mechanisms by which loss of Hectd1 ubiquitin ligase function could lead to the increased density of the cephalic mesoderm observed in *opm* mutant embryos. Together these data indicate that neural fold elevation requires that the amount of head mesenchyme be carefully balanced; either too much (*opm* mutants) or too little (*Twist* and *CART1* mutants) head mesenchyme can lead to a failure of neural fold elevation and neural tube closure.

opm mutant embryos also display a lack of dorsal-lateral hinge point formation in the cranial neural tube, although formation of the medial hinge point appears normal. With respect to the cranial neural tube, it is known that dorsal-lateral hinge point formation is essential for neural fold elevation; however the mechanisms that regulate dorsal-lateral hinge point formation are unknown. Some potential mechanisms could be extrapolated from our knowledge of dorsal-lateral hinge point formation in the spinal neural tube; however these mechanisms have not been determined experimentally for cranial neurulation. In the spinal neural tube there are two described mechanisms that contribute to formation of the dorsal-lateral hinge points. First, Shh signaling inhibits formation of the dorsal-lateral hinge points (Ybot-Gonzalez et al., 2002). In the anterior regions of the spinal neural tube, dorsal-lateral hinge point formation is inhibited by robust Shh signals from the notochord and floorplate. In contrast, in the more caudal regions of the spinal neural tube, Shh signals from the notochord and floorplate diminish allowing the formation of dorsal-lateral hinge points. Failure of this mechanism does not likely play a role in *opm* mutants as our data indicate that there are no obvious changes in dorsal-ventral patterning of the anterior neural tissue in *opm* mutants (data not shown), consistent with normal levels of Shh signaling. Second, in the spinal neural tube, contact with the surface ectoderm is required for induction of the dorsal-lateral hinge points (Hackett et al., 1997). If this mechanism also plays a role in induction of the dorsal-lateral hinge points in the cranial neural tube, then it is possible that the overexpansion of head mesenchyme in *opm* mutant embryos around the neural tube could interfere with this inductive interaction. Indeed, in *opm* mutants the surface ectoderm is greatly separated from the cranial neural tube (Figure 2), suggesting that contact between these two tissues could be required for dorsal-lateral hinge point formation in the cranial regions of the neural tube. Alternatively, it is possible that the denser head mesenchyme simply causes mechanical inhibition of neural fold elevation.

While we detected a defect in the development of the head mesenchyme associated with cranial neural tube closure defects in *opm* mutant embryos it is still a distinct possibility that Hectd1 is also required in other cell lineages for neural tube closure. Our analysis of the expression of Hectd1 indicates that the transcript is also expressed in the neural and non-neural ectoderm during neural tube closure. Therefore, further experiments such as tissue specific deletion of *Hectd1* or chimeric analysis are needed to determine if expression of *Hectd1* in these tissues

also contributes to the lack of dorsal-lateral hinge point formation and the subsequent failure to close the cranial neural tube in *opm* mutant embryos.

Ubiquitination and regulation of development

In recent years, the importance of posttranslational modification of proteins by ubiquitin during embryonic development has become increasingly apparent. Ubiquitination results in the conjugation of a 76 amino acid polypeptide (ubiquitin) to substrate proteins (Kerscher et al., 2006). Polyubiquitination targets proteins for destruction in the proteasome, while monoubiquitination results in the modification of protein function and/or processing. Ubiquitination is a multistep process where an Ubiquitin-activating enzyme (E1) activates ubiquitin and transfers it to an ubiquitin-conjugating enzyme (E2). The E3 ubiquitin ligase associates with both the E2 enzyme and the target substrate through protein-protein interaction domains. There are two main types of ubiquitin ligases: ones that contain a Ring domain and ones that contain a C-terminal HECT (homologous to E6-AP carboxy terminal) domain, the latter type includes Hectd1. The substrate specificity of the ubiquitin pathway arises from the interaction of the E3 ligases with their substrates and the HECT domain ligases interact directly with their substrates.

The *opm* mutation occurs in a gene encoding a novel E3 ubiquitin ligase, Hectd1. Gene identification was confirmed by failure of complementation with the genetrap allele ($Hectd1^{XC}$) in which the HECT domain was disrupted. Additionally, the identical phenotypes observed in mutant embryos homozygous for the $Hectd1^{opm}$ (presumed null) and $Hecd1^{XC}$ alleles indicate that ubiquitin ligase activity is essential for the function of Hectd1 in vivo. The observation that mutation of Hectd1 results in the *opm* phenotype suggests that posttranslational modification of an unknown substrate protein(s) is required for normal development of the head mesenchyme. Since we find that the head mesenchyme around the neural tube is denser as early as E8.5, and that no significant difference in proliferation rates in the head mesenchyme are observed between wildtype and mutant embryos at this stage, expansion of the head mesenchyme could be due to misregulation of the numbers of progenitor cells specified in the primitive streak, the origin of the cephalic mesoderm. As an example, it is possible that *Hectd1* normally regulates a pathway that is required for patterning of the primitive streak, for instance by regulating the strength and/or duration of a patterning signal. Therefore, in this situation, loss of ubiquitin modification by *Hectd1* in *opm* mutants could result in abnormal signaling and an increase in the number of cephalic mesoderm precursors set aside in the primitive streak. Alternatively, it is possible that the apparent expansion of the head mesenchyme is due to a failure to reorganize during neural tube closure. Since the increased density of head mesenchyme indicates that the extracellular space between the mesenchymal cells is also not increased appropriately, it is possible that Hectd1 could regulate the quantity or quality of the extracellular matrix required for reorganization of the head mesenchyme.

Determination of the substrate(s) of the Hectd1 ubiquitin ligase will also lead to a greater understanding of the mechanisms underlying the neural tube closure defects in *opm* mutants. Currently the substrate(s) of Hectd1 are unknown; however the human orthologue of Hectd1, KIAA1131 was recently identified in yeast two-hybrid screens (Nakayama et al., 2002) and (NCBI accession: AAP13073). In both of these screens, Hectd1 was found to bind Immunoglobulin-like domain containing 1 protein (Igsf1), implicating Igsf1 as a potential Hectd1 substrate. Originally, Igsf1 was identified in a screen for proteins that bound the TGFβ antagonist Inhibin and was thus also named InhBP/p120 (Chong et al., 2000); however, subsequent studies have questioned the ability of InhBP/p120 to modulate Inhibin signaling (Bernard et al., 2003; Chapman et al., 2002). The future identification of Hectd1 substrates and their modification by ubiquitination will increase our understanding of the molecular pathways

that regulate the normal (and abnormal) development of the cephalic mesoderm and neural tube closure and provide further molecular insight into the etiology of the *opm* phenotype.

Variable expressivity of neural tube defects in Hectd1 heterozygotes suggests a candidate susceptibility gene locus

Embryos heterozygous for the *opm* allele (presumed null) display a low frequency (~5%) neural tube defects. This suggests that the level of Hectd1 function is critical and that loss of one allele can decrease protein function below a critical threshold. Interestingly, embryos heterozygous for the gene trap allele (*Hectd1*^{XC}) in which the C-terminal HECT domain is disrupted display a higher frequency (~20%) of neural tube defects. It has been shown that mutation of a conserved cysteine in the HECT domain results in a dominant-negative protein by maintaining the interaction of the ligase with the substrate but preventing ubiquitination (Huibregtse et al., 1995; Talis et al., 1998). Thus, the *Hectd1*^{XC} allele could create a dominant-negative protein that prevents interaction of the wildtype protein with the substrate, potentially explaining the higher frequency of neural tube defects in the XC heterozygotes relative to the *opm* allele.

Neural tube closure defects are one of the most common birth defects in humans with approximately one in one thousand live births affected. It is likely that in some cases the genetic factors contributing to human neural tube defects result from a low penetrance of neural tube defects in heterozygous individuals with null or dominant negative mutations in genes that are required for neural tube closure (Harris and Juriloff, 2006). Therefore, it is of interest that Hectd1 heterozygotes display variable expressivity of neural tube defects in heterozygous individuals. Our observations that Hectd1 function is required at a critical threshold level suggest Hectd1 would be a good candidate for a susceptibility gene contributing to neural tube closure defects in humans.

Acknowledgments

We are grateful to Trevor Williams and members of the Niswander and Anderson laboratories for helpful discussions and suggestions, Karen Sears for statistical analysis and Trevor Williams for critical reading of the manuscript. We also thank Lori Bulwith and Andrew Pollock for technical assistance. ES cells used to generate *Hectd1*^{XC} mutant mice were from BayGenomics. This work was supported by NIH grants F32-HD08605 to IEZ, U01-HD43478 and R01-HD035455 to KVA. LAN is a HHMI investigator.

References

Bernard DJ, Burns KH, Haupt B, Matzuk MM, Woodruff TK. Normal reproductive function in InhBP/p120-deficient mice. Mol Cell Biol 2003;23:4882–91. [PubMed: 12832474]

Brewer S, Feng W, Huang J, Sullivan S, Williams T. Wnt1-Cre-mediated deletion of AP-2alpha causes multiple neural crest-related defects. Dev Biol 2004;267:135–52. [PubMed: 14975722]

Caspary T, Anderson KV. Patterning cell types in the dorsal spinal cord: what the mouse mutants say. Nat Rev Neurosci 2003;4:289–97. [PubMed: 12671645]

Chapman DL, Garvey N, Hancock S, Alexiou M, Agulnik SI, Gibson-Brown JJ, Cebra-Thomas J, Bollag RJ, Silver LM, Papaioannou VE. Expression of the T-box family genes, Tbx1-Tbx5, during early mouse development. Dev Dyn 1996;206:379–90. [PubMed: 8853987]

Chapman SC, Bernard DJ, Jelen J, Woodruff TK. Properties of inhibin binding to betaglycan, InhBP/p120 and the activin type II receptors. Mol Cell Endocrinol 2002;196:79–93. [PubMed: 12385827]

Chen ZF, Behringer RR. Twist is required in head mesenchyme for cranial neural tube morphogenesis. Genes Dev 1995;9:686–99. [PubMed: 7729687]

Chong H, Pangas SA, Bernard DJ, Wang E, Gitch J, Chen W, Draper LB, Cox ET, Woodruff TK. Structure and expression of a membrane component of the inhibin receptor system. Endocrinology 2000;141:2600–7. [PubMed: 10875264]

Copp AJ. Neurulation in the cranial region--normal and abnormal. J Anat 2005;207:623–35. [PubMed: 16313396]

Copp AJ, Greene ND, Murdoch JN. The genetic basis of mammalian neurulation. Nat Rev Genet 2003;4:784–93. [PubMed: 13679871]

Crossley PH, Martin GR. The mouse Fgf8 gene encodes a family of polypeptides and is expressed in regions that direct outgrowth and patterning in the developing embryo. Development 1995;121:439–51. [PubMed: 7768185]

Danielian PS, Muccino D, Rowitch DH, Michael SK, McMahon AP. Modification of gene activity in mouse embryos in utero by a tamoxifen-inducible form of Cre recombinase. Curr Biol 1998;8:1323–6. [PubMed: 9843687]

Garcia-Garcia MJ, Eggenschwiler JT, Caspary T, Alcorn HL, Wyler MR, Huangfu D, Rakeman AS, Lee JD, Feinberg EH, Timmer JR, Anderson KV. Analysis of mouse embryonic patterning and morphogenesis by forward genetics. Proc Natl Acad Sci U S A 2005;102:5913–9. [PubMed: 15755804]

Gelineau-van Waes J, Finnell RH. Genetics of neural tube defects. Semin Pediatr Neurol 2001;8:160–4. [PubMed: 11575845]

Hackett DA, Smith JL, Schoenwolf GC. Epidermal ectoderm is required for full elevation and for convergence during bending of the avian neural plate. Dev Dyn 1997;210:397–406. [PubMed: 9415425]

Harris MJ, Juriloff DM. Mouse mutants with neural tube closure defects and their role in understanding human neural tube defects. Birth Defects Res A Clin Mol Teratol. 2006

Hildebrand JD, Soriano P. Shroom, a PDZ domain-containing actin-binding protein, is required for neural tube morphogenesis in mice. Cell 1999;99:485–97. [PubMed: 10589677]

Hogan, B.; Beddington, RS.; Costantini, F.; Lacy, E. Manipulating the Mouse Embryo, a Laboratory Manual. Cold Spring Harbor Laboratory Press; 1994.

Holmes G, Niswander L. Expression of slit-2 and slit-3 during chick development. Dev Dyn 2001;222:301–7. [PubMed: 11668607]

Huibregtse JM, Scheffner M, Beaudenon S, Howley PM. A family of proteins structurally and functionally related to the E6-AP ubiquitin-protein ligase. Proc Natl Acad Sci U S A 1995;92:5249. [PubMed: 7761480]

Jones CM, Lyons KM, Hogan BL. Involvement of Bone Morphogenetic Protein-4 (BMP-4) and Vgr-1 in morphogenesis and neurogenesis in the mouse. Development 1991;111:531–42. [PubMed: 1893873]

Kasarskis A, Manova K, Anderson KV. A phenotype-based screen for embryonic lethal mutations in the mouse. Proc Natl Acad Sci U S A 1998;95:7485–90. [PubMed: 9636176]

Kaufman, MH.; Bard, JBL. The Anatomical Basis of Mouse Development. Academic Press; San Diego: 1999.

Kerscher O, Felberbaum R, Hochstrasser M. Modification of Proteins by Ubiquitin and Ubiquitin-Like Proteins. Annu Rev Cell Dev Biol. 2006

Liu A, Joyner AL, Turnbull DH. Alteration of limb and brain patterning in early mouse embryos by ultrasound-guided injection of Shh-expressing cells. Mech Dev 1998;75:107–15. [PubMed: 9739117]

Mitchell PJ, Timmons PM, Hebert JM, Rigby PW, Tjian R. Transcription factor AP-2 is expressed in neural crest cell lineages during mouse embryogenesis. Genes Dev 1991;5:105–19. [PubMed: 1989904]

Morriss GM, Solursh M. Regional differences in mesenchymal cell morphology and glycosaminoglycans in early neural-fold stage rat embryos. J Embryol Exp Morphol 1978;46:37–52. [PubMed: 702034]

Nakayama M, Kikuno R, Ohara O. Protein-protein interactions between large proteins: two-hybrid screening using a functionally classified library composed of long cDNAs. Genome Res 2002;12:1773–84. [PubMed: 12421765]

Nieto MA, Bennett MF, Sargent MG, Wilkinson DG. Cloning and developmental expression of Sna, a murine homologue of the Drosophila snail gene. Development 1992;116:227–37. [PubMed: 1483390]

Noden DM, Trainor PA. Relations and interactions between cranial mesoderm and neural crest populations. J Anat 2005;207:575–601. [PubMed: 16313393]

Pusch C, Hustert E, Pfeifer D, Sudbeck P, Kist R, Roe B, Wang Z, Balling R, Blin N, Scherer G. The SOX10/Sox10 gene from human and mouse: sequence, expression, and transactivation by the encoded HMG domain transcription factor. Hum Genet 1998;103:115–23. [PubMed: 9760192]

Schatteman GC, Morrison-Graham K, van Koppen A, Weston JA, Bowen-Pope DF. Regulation and role of PDGF receptor alpha-subunit expression during embryogenesis. Development 1992;115:123–31. [PubMed: 1322269]

Schorle H, Meier P, Buchert M, Jaenisch R, Mitchell PJ. Transcription factor AP-2 essential for cranial closure and craniofacial development. Nature 1996;381:235–8. [PubMed: 8622765]

Skarnes WC, von Melchner H, Wurst W, Hicks G, Nord AS, Cox T, Young SG, Ruiz P, Soriano P, Tessier-Lavigne M, Conklin BR, Stanford WL, Rossant J. A public gene trap resource for mouse functional genomics. Nat Genet 2004;36:543–4. [PubMed: 15167922]

Soriano P. Generalized lacZ expression with the ROSA26 Cre reporter strain. Nat Genet 1999;21:70–1. [PubMed: 9916792]

Talis AL, Huibregtse JM, Howley PM. The role of E6AP in the regulation of p53 protein levels in human papillomavirus (HPV)-positive and HPV-negative cells. J Biol Chem 1998;273:6439–45. [PubMed: 9497376]

Timmer JR, Wang C, Niswander L. BMP signaling patterns the dorsal and intermediate neural tube via regulation of homeobox and helix-loop-helix transcription factors. Development 2002;129:2459–72. [PubMed: 11973277]

Ybot-Gonzalez P, Cogram P, Gerrelli D, Copp AJ. Sonic hedgehog and the molecular regulation of mouse neural tube closure. Development 2002;129:2507–17. [PubMed: 11973281]

Zhang J, Hagopian-Donaldson S, Serbedzija G, Elsemore J, Plehn-Dujowich D, McMahon AP, Flavell RA, Williams T. Neural tube, skeletal and body wall defects in mice lacking transcription factor AP-2. Nature 1996;381:238–41. [PubMed: 8622766]

Zhao Q, Behringer RR, de Crombrugghe B. Prenatal folic acid treatment suppresses acrania and meroanencephaly in mice mutant for the Cart1 homeobox gene. Nat Genet 1996;13:275–83. [PubMed: 8673125]

Zohn IE, Anderson KV, Niswander L. Using genomewide mutagenesis screens to identify the genes required for neural tube closure in the mouse. Birth Defects Res A Clin Mol Teratol. 2005

Zoltewicz JS, Stewart NJ, Leung R, Peterson AS. Atrophin 2 recruits histone deacetylase and is required for the function of multiple signaling centers during mouse embryogenesis. Development 2004;131:3–14. [PubMed: 14645126]

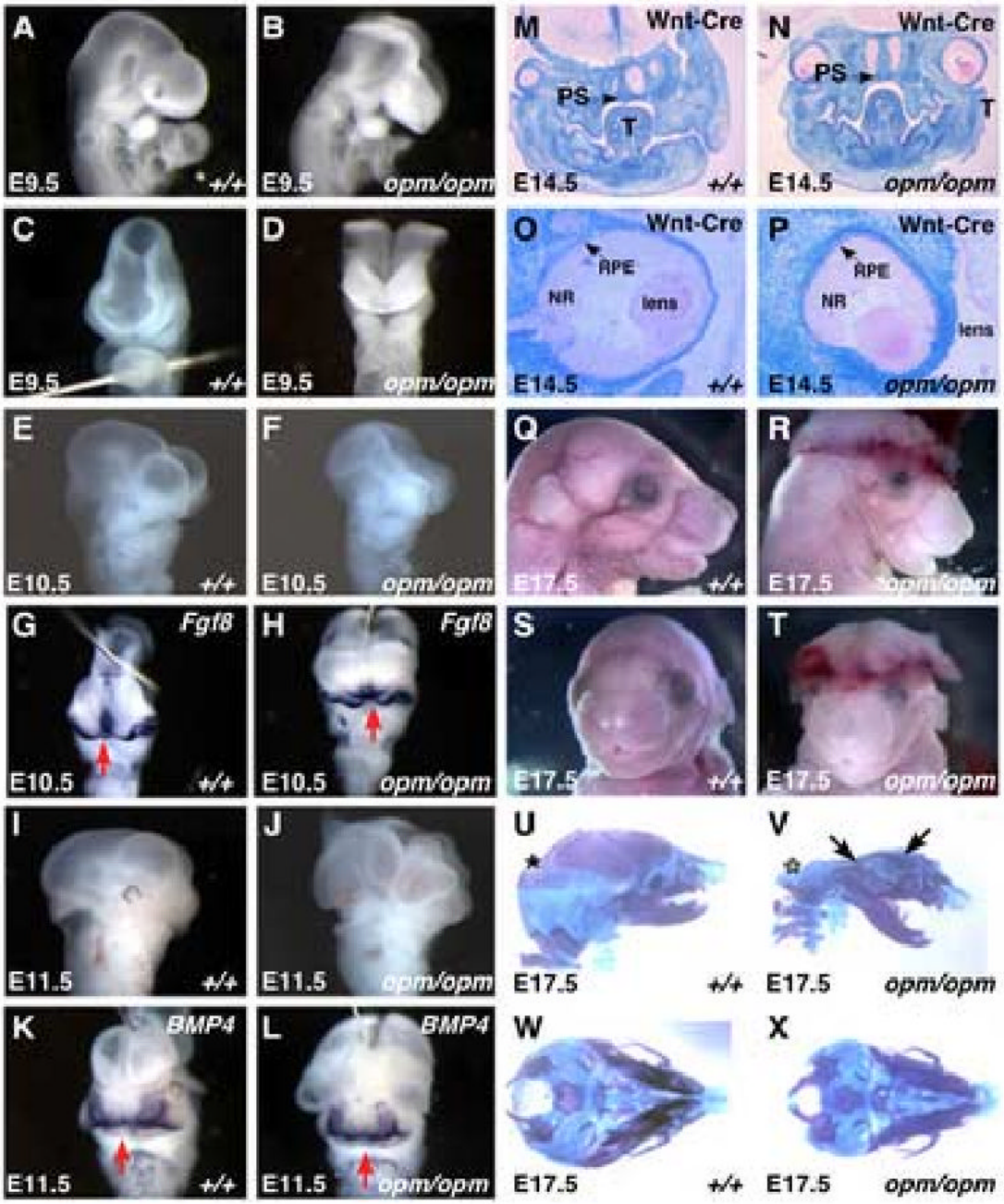

Figure 1. *opm* mutant embryos exhibit defects in neural tube closure without other significant defects in craniofacial development

Panels A-L: lateral (A, B, E, F, I and J) and frontal (C, D, G, H, K and L) views of wildtype (A, C, E, G, I and K) and *opm* mutant (B, D, F, H, J, L) heads demonstrating neural tube closure defect from the forebrain to the hindbrain and normal development of the face (A-D, E9.5; E-H, E10.5; I-L, E11.5). Frontal views of wildtype and *opm* mutant embryos at E10.5 and E11.5 were labeled by in situ hybridization using probes against *Fgf8* and *BMP4* respectively to highlight the developing frontal nasal processes. Fate of the neural crest as shown in coronal sections of E14.5 Wnt1-Cre/R26R wildtype (M,O) and *opm* mutant (N,P) embryos stained for β-galactosidase activity and counterstained with eosin. Arrow points to the properly fused

secondary palatal shelves (PS; T=Tongue) in wildtype (M) and *opm* mutant (N) heads. Eye development is abnormal in *opm* mutant embryos (P). The retinal pigmented epithelium (RPE, arrow), neural retina (NR) and lens appear histologically normal, but eyes are rotated in the head of *opm* mutant embryos. Profile (Q,R) and frontal (S,T) views of E17.5 wildtype (Q,S) and *opm* mutant (R,T) heads demonstrating normal craniofacial development in spite of the severe neural tube closure defect. Lateral (U,V) and basal (W,X) views of E17.5 skeletal preparations stained with Alcian blue and Alizarin Red in wildtype (U,W) and *opm* mutant (V,X) skulls. Asterisk (*) denotes exoccipital, petrosal and interpariatal bones that are missing in *opm* mutant skulls. Arrows point to frontal and pariatal bones that are malformed in *opm* mutant skulls.

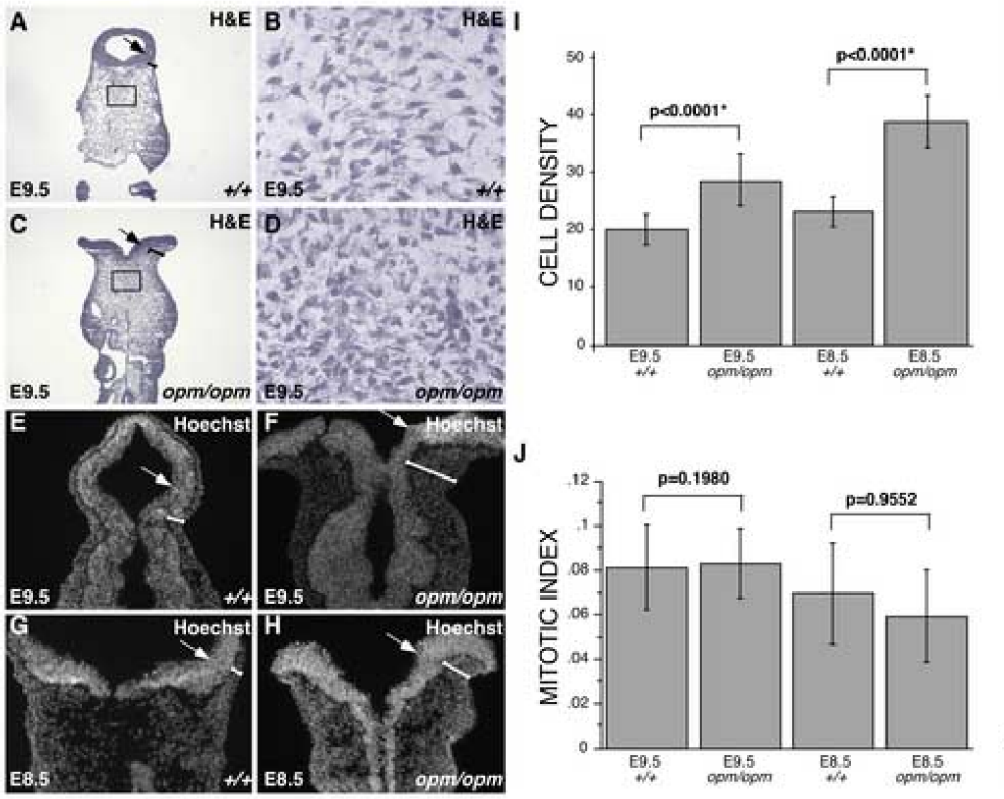

Figure 2. Abnormal head mesenchyme development in *opm* mutant embryos is associated with neural tube closure defects

A-D. Hematoxylin and Eosin (H&E) staining of coronal sections of wildtype (A,B) and *opm* mutant (C,D) heads at E9.5. Brackets highlight the region of head mesenchyme that are expanded around the *opm* neural tube. Panels B&D show magnified views of the boxes drawn in panels A&C, demonstrating the abnormally dense cellular organization of *opm* mutant head mesenchyme. E-H. Nuclei were visualized by staining with Hoechst in coronal sections of wildtype (E,G) and *opm* mutant (F,H) at E9.5 (E,F) and E8.5 (G,H) demonstrating that the head mesenchyme is denser around the dorsal neural tube of *opm* mutant embryos during neurulation. There is also a failure of dorsal-lateral hinge point formation leading to a flat or convex curvature of the *opm* neural tube compared to the concave neural tube in wildtype embryos at both stages. Arrows point to dorsal-lateral hinge points in A-H. I. Cell density was determined by counting the number of nuclei in 1-2 defined areas on many sections from many embryos (E9.5: wildtype n=39 areas, *opm* mutant n=41 areas; E8.5: wildtype n=58 areas, *opm* mutant n=63 areas). Error bars represent one standard deviation from the mean. The density of cells between wildtype and *opm* mutant samples are significantly different as calculated by the Mann-Whitney U test (E9.5: P-value<0.0001*; E8.5: P-value<0.0001*). J. Mitotic indexes were calculated by dividing the number of P-H3 positive cells by the number of nuclei in a given area for wildtype and *opm* mutant in two to three sections from many embryos (E9.5: wildtype n=19 sections, *opm* mutant n=20 sections; E8.5: wildtype n=17 sections, *opm* mutant n=18 sections). Error bars represent one standard deviation from the mean. Samples are not significantly different as calculated by the Mann-Whitney U test (E9.5: P-value=0.9552; E8.5: P-value=0.1980).

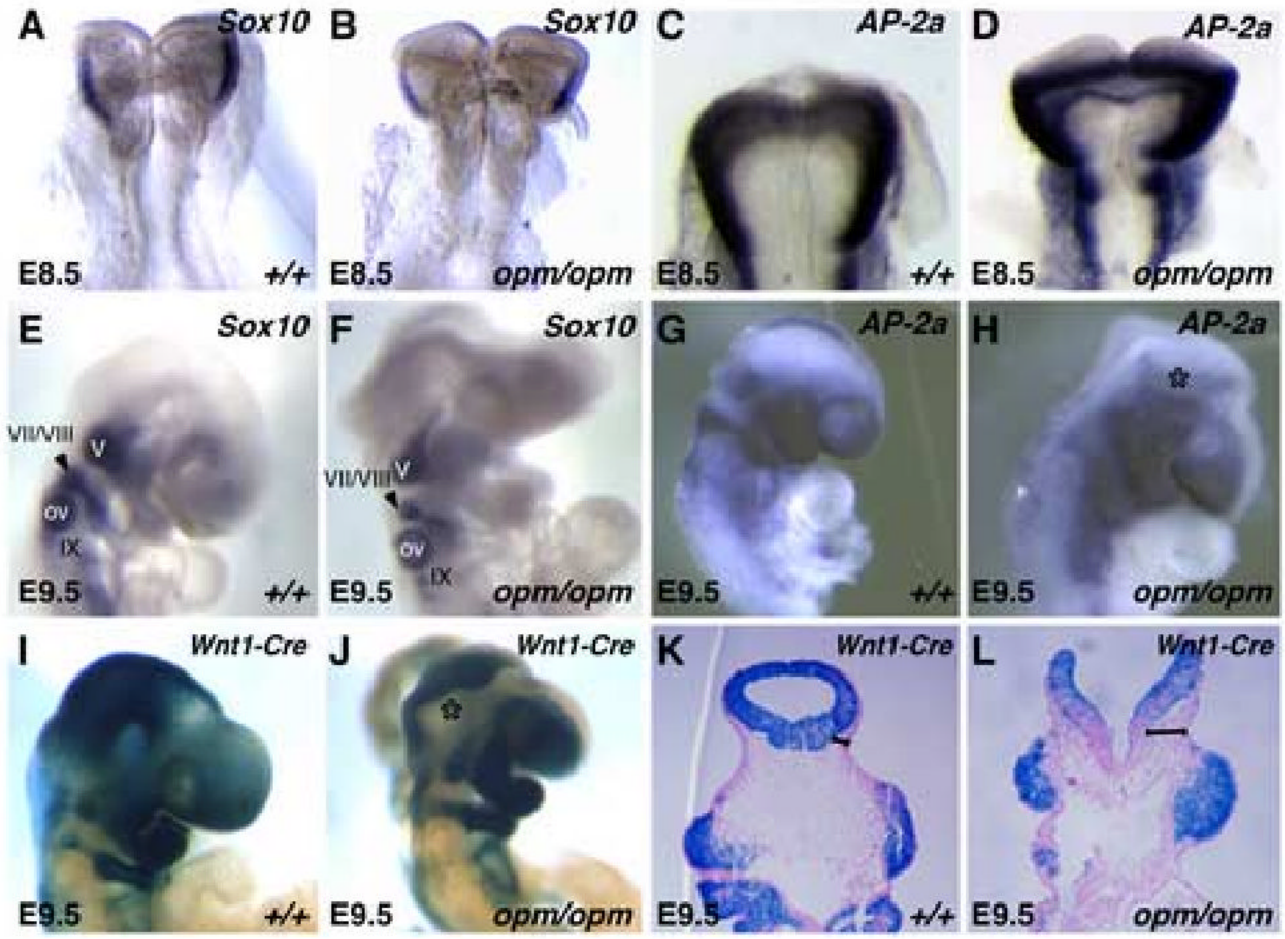

Figure 3. Neural crest cells are not present in the abnormal *opm* mutant head mesenchyme

E8.5 (A-D) and E9.5 (F-H) wildtype (A,C,E,G) and *opm* mutant (B,D,F,H) embryos were analyzed by whole-mount in situ hybridization analysis for expression of *Sox10* (A,B,E,F) and *AP-2α* (C,D,G,H). Asterisk (*) in panel H denotes the lack of *AP-2α* expression in the abnormal head mesenchyme surrounding the open neural tube in the *opm* mutant head. V, VII/VIII and IX denote the *Sox10*-expressing cranial nerves. OV = otic vesicle. Fate of the neural crest in E9.5 Wnt1-Cre/R26R wildtype (I) and *opm* mutant (J) embryos that were stained in whole-mount for β-galactosidase activity. Asterisk (*) highlights the abnormal head mesenchyme in *opm* mutant embryos that is negative for β-galactosidase activity. Coronal sections of E9.5 Wnt1-Cre/R26R wildtype (K) and *opm* mutant (L) head stained for β-galactosidase and counterstained with eosin. Brackets highlight the abnormally expanded head mesenchyme in *opm* mutant embryos that is negative for β-galactosidase activity.

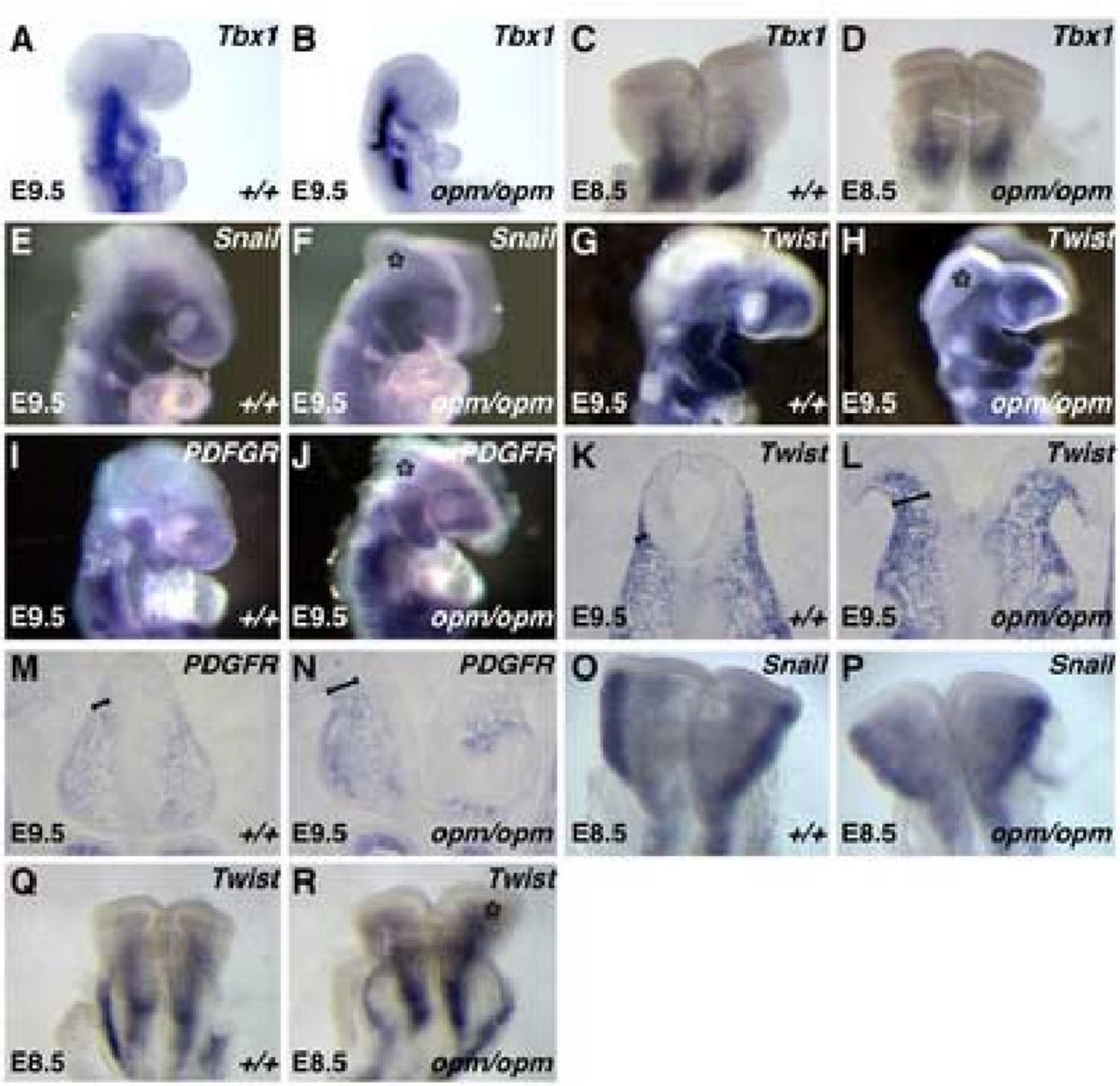

Figure 4. The abnormal head mesenchyme in *opm* mutant embryos expresses molecular markers of cephalic mesoderm

E9.5 (A,B,E,F,G,H,I,J) and E8.5 (C,D,O,P,Q,R) wildtype (A,C,E,G,I,O,Q) and *opm* mutant (B,D,F,H,J,P,R) heads were analyzed by whole-mount in situ hybridization analysis for expression of *Tbx1* (A-D), *Snail* (E,F,O,P), *Twist* (G,H,Q,R) and *PDGFRα* (I,J). Asterisk (*) denotes staining in the abnormal head mesenchyme surrounding the open neural tube in *opm* mutant embryos. Coronal sections of wildtype (K,M) and *opm* mutant (L,N) heads stained by in situ hybridization for expression of *Twist* (K,L) and *PDGFRα* (M,N). Brackets highlight the abnormal head mesenchyme surrounding the open neural tube in *opm* mutant embryos.

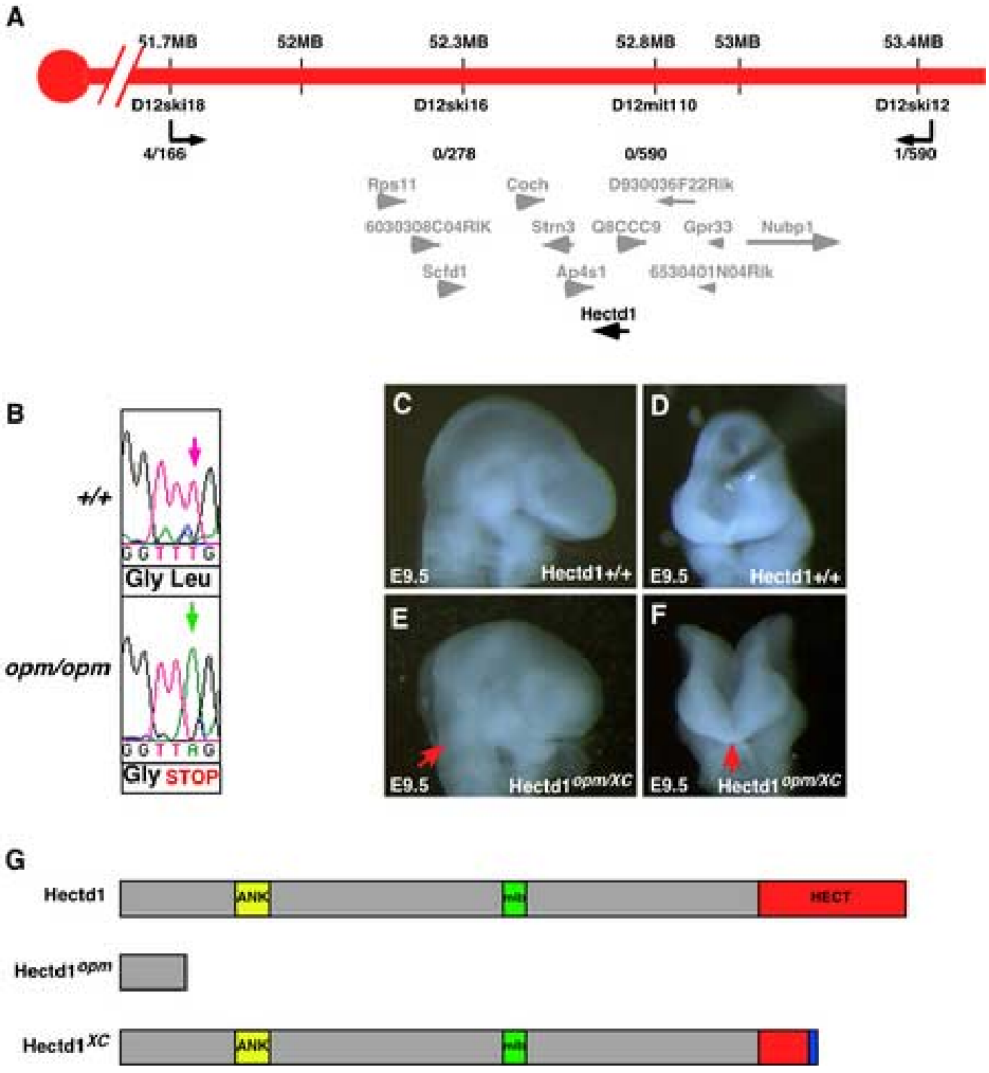

Figure 5. The *opm* mutation disrupts the uncharacterized *Hectd1* ubiquitin ligase

A. Genetic map of *opm* interval on mouse chromosome 12. The number of recombination events over the number of opportunities for recombination is indicated for each polymorphic marker. Markers D12ski16 and D12MIT110 never separated from the *opm* phenotype. Within this interval are twelve transcription units: *Rps11* (ribosomal protein S11), *6030308C04RIK* (RIKEN cDNA 6030408C04 gene), *Scfd1* (sec1 family domain containing 1), *Coch* (coagulation factor C homolog), *Strn3* (striatin, calmodulin binding protein 3), *Ap4s1* (adaptor-related protein complex AP-4, sigma 1), *Hectd1* (HECT domain containing 1), *Q8CCC9* (PREDICTED: hypothetical protein), *D930036F22Rik* (RIKEN cDNA D930036F22 gene), *6530401N04Rik* (RIKEN cDNA 6530401N04 gene), *Gpr33* (G protein-coupled receptor 33) and *Nubp1* (nucleotide binding protein-like). The transcripts in the *opm* interval and physical map position (mb) is from the Ensemble mouse genome assembly release #40. B. The *opm* ENU-induced mutation results in a T to A transversion (green arrow) at position 430 in the *Hectd1* coding sequence. This mutation results in a nonsense mutation changing a Leucine to a stop codon. C-F. The *Hectd1*^{XC} gene trap allele fails to complement *Hectd1*^{opm} as embryos at E9.5 exhibit exencephaly from the hindbrain to the forebrain (E,F). Panels C-F show lateral (C,E) and frontal (D,F) views of wildtype (C,D) and *Hectd1*$^{opm/XC}$ mutant (E,F) E9.5 embryos.

G. Predicted protein motifs in *Hectd1*: an ankyrin domain (ANK), MIB-HERC2 domain (mib) and a C-terminal Homologous to the E6-AP Carboxyl Terminus domain (HECT). The *Hectd1*^{opm} mutation results in a truncated protein at amino acid 145. The *Hectd1*^{XC} mutation results in an insertion and truncation of the HECT domain.

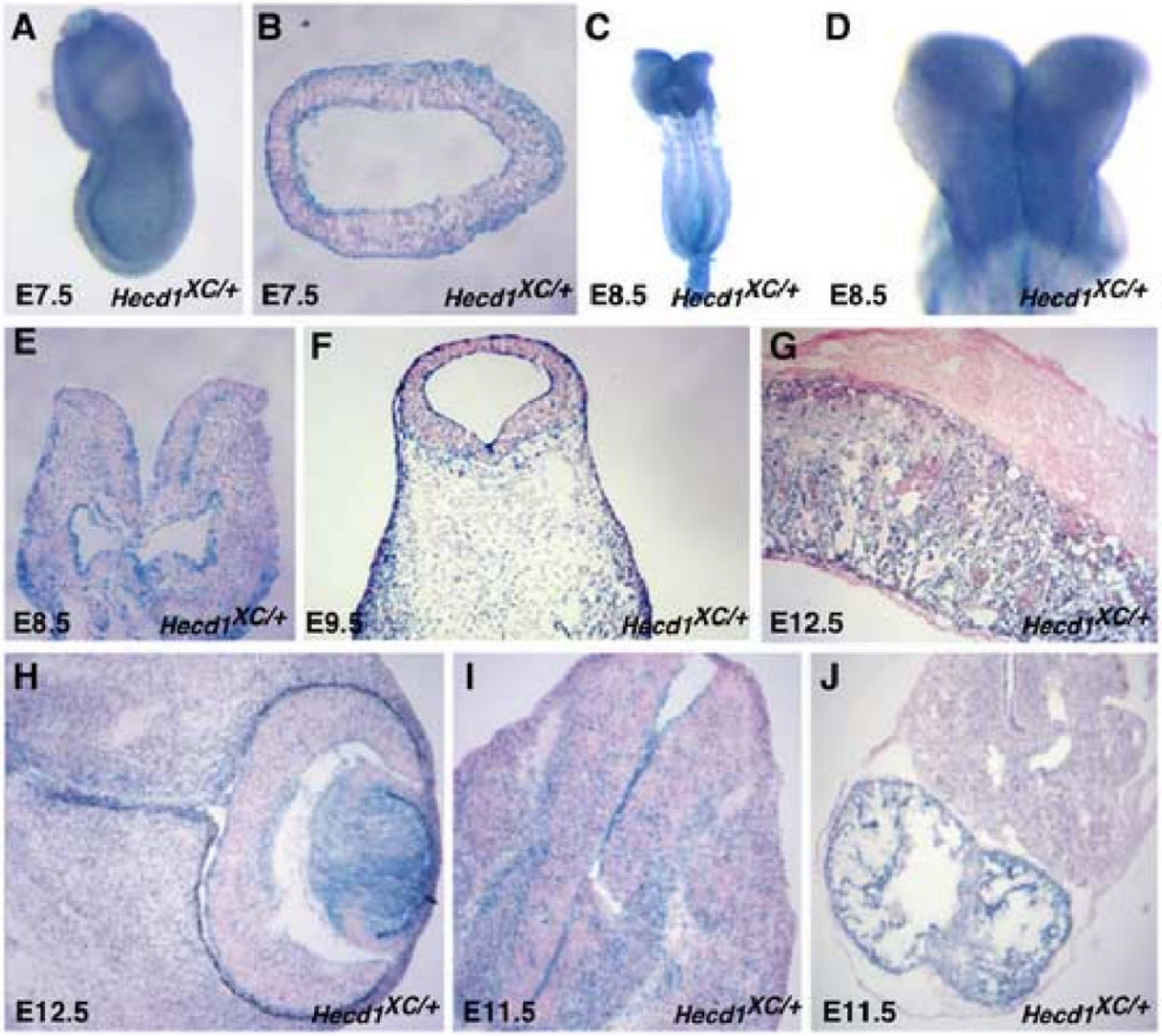

Figure 6. *Hectd1* is ubiquitously expressed during development of the mouse embryo

Hectd1 expression was monitored by staining for β-galactosidase activity in whole mount (A,C,D) or in section and counterstained with eosin (B,E-J) in *Hectd1*$^{XC/+}$ embryos. *Hectd1* is expressed during development of the head mesenchyme at E7.5 (A,B), E8.5 (C-E) E9.5 (F). *Hectd1* is also expressed in the placenta (G) and eye (H) at E12.5. *Hectd1* is expressed at E11.5 at higher levels in differentiated neurons of the developing spinal cord (I) and the atrium of the heart (J).

Table 1

Mendelian rations of *opm/opm* embryos are found upon dissection at E9.5-12.5 and a small percentage of *opm/+* embryos exhibit exencephaly

	Number of embryos					
Age	**+/+**	***opm*/+**	***opm*/*opm***	**Number of embryos with exencephaly**	**Number of *opm*/+ embryos with exencephaly**	**Total number of embryos**
E9.5	81	178	76	86	10	335
E10.5	50	83	43	45	2	176
E11.5	11	31	13	13	0	55
E12.5	4	9	9	11	3	22
Total:	146	301	141	165	15	588
	25%	51%	24%	28%	5%	

Table 2

Hectd1$^{XC/+}$ embryos exhibit exencephaly at a higher frequency than Hecd1$^{opm/+}$ embryos

	Number of embryos					
Age	**+/+**	***XC*/+**	***XC*/*XC***	**Number of embryos with exencephaly**	**Number of *XC*/+ embryos with exencephaly**	**Total number of embryos**
E9.5	9	22	14	18	4	45
E10.5	1	5	0	1	1	6
E11.5	2	10	5	8	3	17
E12.5	2	3	2	2	0	7
Total:	17	40	22	30	8	79
	22%	50%	28%	38%	20%	